Bubble size distribution in dissolved air flotation tanks

D. M. Leppinen and S. B. Dalziel

ABSTRACT

This papers presents the results of two studies performed to measure the size distribution of bubbles at different locations in dissolved air flotation tanks. Measurements were performed at the Albert Water Treatment Works and in two separate tanks at the Graincliffe Water Treatment Works (Yorkshire Water). At Albert, and in one of the tanks at Graincliffe, bubbles were generated using conventional pressure reduction nozzles. Bubbles in the second tank at Graincliffe were generated using needle valves. Bubble size distributions are presented and variations in the size distributions at different locations in the flotation tanks are explained. It is observed that bubble clustering plays an important role in dissolved air flotation and that smaller bubbles are preferentially incorporated into these clusters. Macrobubble formation by the needle valves reduces the efficiency of the flotation process. It is concluded that flotation is enhanced by the use of smaller bubbles.

Key words | bubble clusters, bubble size distribution, dissolved air flotation, field measurements, macrobubbles

D. M. Leppinen (corresponding author)
S. B. Dalziel
Department of Applied Mathematics and Theoretical Physics,
Centre for Mathematical Sciences,
University of Cambridge,
Wilberforce Road,
Cambridge, CB3 0WA
UK
Tel.: +44 (0)1223 337744
Fax: +44 (0)1223 765900
E-mail: *D.M.Leppinen@damtp.cam.ac.uk*

INTRODUCTION

Dissolved air flotation is a separation process which is widely used in water and wastewater treatment. The process uses microscopic air bubbles to remove suspended particles from water. The air bubbles are generated by first saturating water with air at high pressure, and then passing this saturated water through a pressure reduction nozzle. The water is then supersaturated and air comes out of solution in the form of microbubbles. These bubbles then collide with, and become attached to, the suspended particles to form positively buoyant bubble/particle agglomerates. The agglomerates then rise to the top of the flotation tank where they collect in a sludge blanket which can subsequently be removed.

The purpose of this paper is to present the results from a study performed to measure the size distributions of bubbles measured at different locations within full-scale dissolved air flotation tanks. First, a background is given which describes different aspects of the flotation process. This background section will provide the necessary insight to interpret the result of the measurement study. Next, the method used to measure the bubble sizes is presented and then the results are discussed. Finally, it is concluded that the results from the measurement study can be used to suggest ways of increasing the efficiency of dissolved air flotation. The results presented in this paper are thought to be the first direct measurements of bubble size made in a full-scale dissolved air flotation tank.

BACKGROUND

The fundamental act during flotation is the formation of positively buoyant bubble/particle agglomerates. After a flocculation stage, particle-laden water enters the flotation tank and is mixed with a recycle stream which has been saturated with air at high pressure in order to generate microbubbles. The surface chemistry of the flocs is adjusted to promote the attachment of bubbles onto floc particles. Provided they are sufficiently buoyant, the bubble/particle agglomerates will rise to the sludge blanket at the top of the flotation tank. Otherwise the

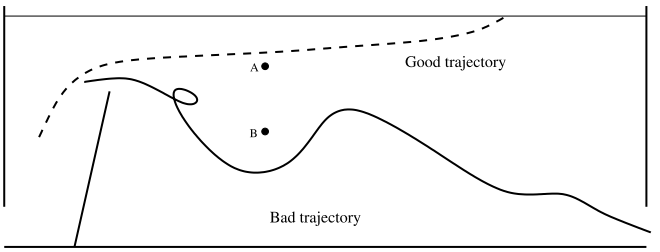

Figure 1 | Schematic of a second generation dissolved air flotation tank. The dashed line represents the path of a bubble/particle agglomerate that leads to successful flotation, the solid line corresponds to unsuccessful flotation.

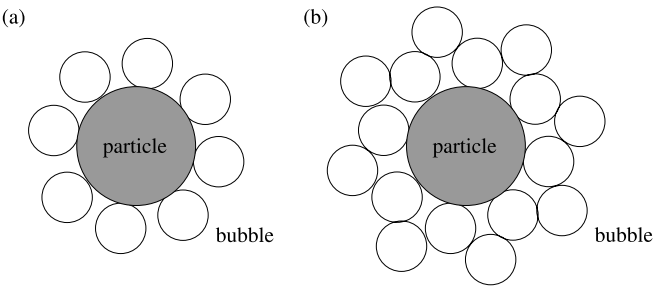

Figure 2 | Possible configurations of bubble/particle agglomerates. The filled circles represent particles and the open circles represent bubbles.

agglomerate will be carried away with the exit flow stream and will ultimately have to be separated using a filtration stage. Efficient flotation will reduce head losses due to filter clogging and will hence increase the time before which the filters will have to be backwashed.

A schematic of a so-called second generation (Kiuru 2001) flotation tank is given in Figure 1. Particle-laden water mixes with the recycle stream in the contact zone of the flotation tank. The buoyancy of the bubble/particle agglomerates is enhanced in the contact zone due to the attachment of bubbles. After exiting the contact zone the agglomerates enter the flotation zone. Figure 1 shows two typical paths for the agglomerate in the flotation zone. The dashed curve corresponds to successful flotation with the agglomerate rising to the sludge blanket and the solid curve corresponds to unsuccessful flotation with a particle being carried away with the exit flow stream. The velocity $\mathbf{v}$ of the agglomerate in the flotation zone can be written as:

$$\mathbf{v} = \mathbf{v}_{\mathrm{rise}} + \mathbf{v}_{\mathrm{mean}} + \mathbf{v}_{\mathrm{turb}} \tag{1}$$

where $\mathbf{v}_{\mathrm{rise}}$ is the rise speed of the agglomerate in an otherwise quiescent environment, $\mathbf{v}_{\mathrm{mean}}$ is the velocity due to the mean flow in the flotation tank and $\mathbf{v}_{\mathrm{turb}}$ is the velocity due to turbulent fluctuations. The mean flow in the tank is downwards towards the tank exit and the turbulent component will cause agglomerates to move both upwards and downwards at different points in the flotation zone. To ensure that an agglomerate can rise to the sludge blanket, $\mathbf{v}_{\mathrm{rise}}$ should be made as large as possible.

Matsui *et al.* (1998), Fukushi *et al.* (1998) and Leppinen (2000) have used kinetic models in order to predict the rise speed of agglomerates during flotation. This rise speed will depend on a number of factors including the bubble size, the particle size and density, the number density of bubbles and flocs in the contact zone and the residence time of fluid within the contact zone. For example, Figure 2 shows some possible (highly idealized) bubble/particle agglomerates with a different number of bubbles attached to each particle. Assuming floc particles of equal size and density, the agglomerate in Figure 2(a) would have a higher rise velocity than the agglomerate in Figure 2(b), and it would clearly be desirable to produce agglomerates similar to those in Figure 2(a). That said, it is the conditions in the contact zone which will determine whether it is the agglomerate in Figure 2(a) or in Figure 2(b), or indeed, if any other agglomerate is formed. The purpose of this paper is not to model the formation of bubble/particle agglomerates. Instead, observations of actual bubble/particle agglomerates will be discussed, and these observations will be used to hypothesize mechanisms which enhance the rise speed of agglomerates. The results presented in this paper identify the dominant processes in a flotation tank and should thus be of great benefit to future modellers of bubble/floc particle agglomeration.

For the study described in this paper, measurements were performed at a number of different locations in the flotation tank. In particular, instead of following the paths of individual bubbles or agglomerates (such as the curves in Figure 1), observations were made of the bubbles or

agglomerates which passed through a fixed point (such as point A or B in Figure 1) during a given time interval. The measurement point B in Figure 1 is at the same downstream location as the measurement point A, but it is at a greater depth. Following the discussion of Equation (1) above, it can be argued that the probability of finding an agglomerate or a bubble with a large rise velocity at point A should be larger than the probability at point B. Indeed, the probability of finding bubbles or agglomerates at a given depth should be inversely related to the rise velocity of the bubble or agglomerate, with agglomerates with a large rise velocity less likely to be found at a greater depth. This physically intuitive hypothesis is significant because it will be used to help interpret the results from the measurement study and to identify factors which can be used to enhance flotation efficiency.

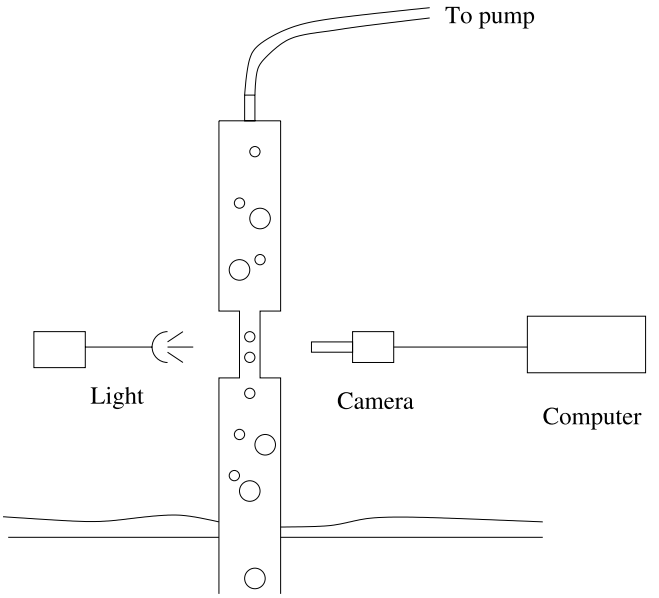

Figure 3 | Schematic of bubble size distribution instrumentation.

METHOD

Bubble size measurements were performed at two dissolved air flotation treatment works operated by Yorkshire Water. A preliminary measurement study was performed at the Albert Water Treatment Works. The purpose of this study was to test the bubble size measurement instrumentation and to collect baseline data. A second measurement study was performed at the Graincliffe Water Treatment Works. At Graincliffe measurements were performed in two flotation tanks. Tank A was fitted with the same type of pressure reduction nozzle that was used at Albert (hereafter referred to as the Albert nozzle). The design of this nozzle is discussed by Franklin *et al.* (1997). Tank B was fitted with needle valves. Hence the Graincliffe study provided a unique opportunity to study two different bubble generation techniques in otherwise identical conditions. The plant layout at Graincliffe also made it possible to observe the size of flocs before they entered the flotation tanks.

Measurements were made by inserting a perspex tube vertically into the flotation tank at a desired location. A pump is then used to draw samples of bubble/floc-laden water and these samples are viewed through a viewing window in the cylinder (see Figure 3). The tube had an internal diameter of 11.5 cm, and the length of the tube varied (by bolting on additional segments) from 2.2 m to 4.2 m depending on the depth of the measurement point. The viewing window is back-lit and the images are recorded using a high resolution digital video camera (JAI Model CV/M4-CL) fitted with a 0.75 × to 4.5 × macro zoom lens. The CV/M4-CL is a monochrome CCD camera with 1,280 (horizontal) by 1,024 (vertical) pixels digitized at 8 bits. At the maximum magnification used for all bubble size measurements, the pixel resolution is 1.4 by 1.4 μm. The digital images were stored on a PC and were subsequently analysed using the DigiFlow (Dalziel 2003) image processing system. A bubble sizing algorithm (Leppinen & Dalziel 2003) has been developed to automatically measure bubble sizes in the digital images. Typically 2000 or more bubbles were used to determine the bubble size distribution.

The perspex tube was held in place using an aluminium traverse framework so that measurements could be made at virtually any location within the flotation tank with the measurement point corresponding to the location of the bottom of the perspex tube. The use of a perspex tube/pump configuration was necessitated by the desire not to immerse the camera into the flotation tank.

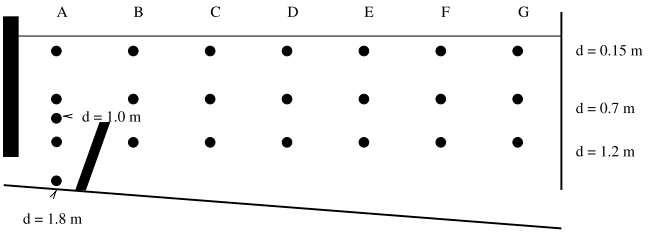

Figure 4 | Location of the measurement points during the Albert study.

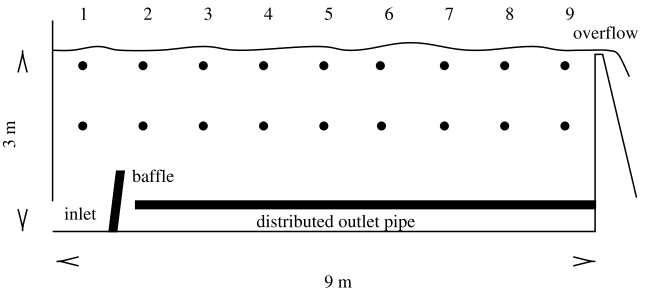

Figure 5 | Location of the measurement points during the Graincliffe study.

While there are submersible video cameras, none is suitable for use with a macro lens of sufficient magnification to view bubbles and flocs. The primary assumption is that bubbles and flocs are not influenced by flow within the perspex tube. To verify this measurements were performed at different pump flow rates ranging from 0.5 to 4 l min^{-1} (corresponding to flow velocities in the bubble tube ranging from 0.08 cm s^{-1} to 0.64 cm s^{-1}). The results show that the measurements were indeed independent of flow rate (i.e. bubble size distributions measured at the same measurement point were equal, for all flow rates investigated). While it is possible that bubbles may coalesce within the tube, it is felt that the turbulence levels within the tube are lower than those in the flotation tank, and hence, if anything, bubble coalescence should be suppressed. To minimize the in fluence of the sidewalls of the perspex tube the camera was focused 1 cm to the interior of the viewing window.

A cross-section of the flotation tank at Albert is given in Figure 4. The tank is approximately 7 m wide, 7 m long (from inlet to outlet) and varies in depth from 1.8 m to 2.4 m as shown. Measurements were performed at the points indicated at four separate locations across the width of the tank. The results were seen to be independent of the distance from the sidewall of the tank and, consequently, all measurements have been averaged across the width of the tank. The Albert flotation tank was hydraulically desludged periodically via an over flow weir at the downstream end of the tank.

A cross-section of the flotation tanks at Graincliffe is given in Figure 5. The Graincliffe tanks are relatively long (9 m), narrow (4 m) and deep (3 m) in comparison with the Albert tank. There is a short (approximately 1 m) steep baffle near the inlet, and there are a series of four horizontal perforated pipes along the base of the tank downstream of the baffle which act as a distributed sink for the outlet flow stream. The Graincliffe tanks were continuously desludged with a rotating scrapper located at the downstream end of the tank.

RESULTS AND DISCUSSION

Albert study

The preliminary study at Albert provided valuable insight into the flotation process. The most striking observation was a phenomenon we have termed bubble clustering (see Figure 6). The dark circles with a bright central spot are microbubbles which are in focus. It can be seen that the bubbles cluster together into large groups with floc particles clumped between the bubbles. The large buoyancy of a cluster as a whole ensures that the cluster will have a much greater rise velocity than an individual bubble. As clusters rise, it is hypothesized, they act as a net, collecting smaller clusters and/or floc particles which have not yet attached to bubbles. While the temporal resolution from the video camera was too slow to see bubble clusters acting as nets, the image in Figure 6 and images of thousands of other bubble clusters are consistent with this hypothesis. This is of significance because it implies that the buoyancy of bubble particle agglomerates can change while in the flotation zone as well as in the contact zone of a flotation tank. The bubble clusters in Figure 6 are significantly more complex than the idealized agglomerates in Figure 2. Nevertheless, it is clear that kinetic models such

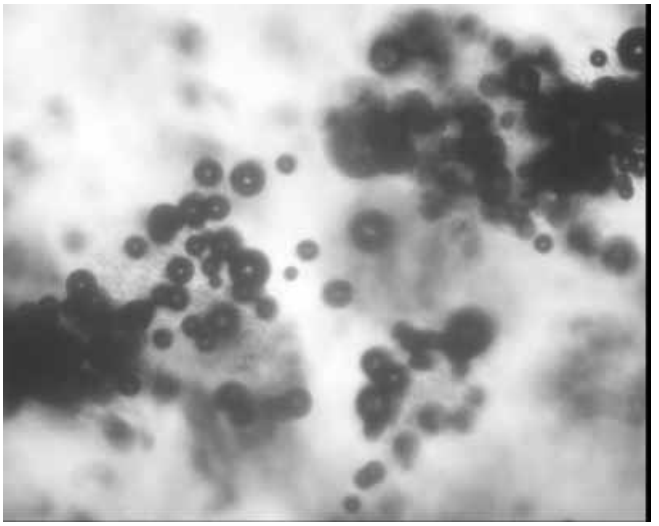

Figure 6 | A magnified image of bubble clusters. The image is 1.8 mm wide by 1.5 mm high.

as those by Matsui *et al*. (1998), Fukushi *et al*. (1998) and Leppinen (2000) which allow for multiple bubble attachment onto flocs are significantly more realistic than models which only consider one bubble interacting with one particle (Han & Lawler 1991; Han *et al*. 1997; Leppinen 1999).

At each measurement location in Albert 1,000 images were recorded. The average number of clusters per image at each location is tabulated in Table 1. It is observed that bubble clusters are rarely seen at depth in the flotation zone. Since it is clear that clusters do form, the fact that they do not sink to depth in the flotation zone implies that they must be rising to the sludge layer. By acting as nets as they rise, bubble clusters can collect significantly larger amounts of flocs than individual bubbles. Indeed, the images collected at Albert suggest that bubble clusters essentially act as filters, and that clusters, as opposed to isolated bubbles, are the primary means for floc removal during flotation. The fact that the number of bubble clusters measured at a depth of 0.15 m decreases away from the contact zone provides further evidence that bubble clustering leads to successful flotation.

Given the importance of bubble clusters, it seems logical to question: Which size of bubble should be generated during dissolved air flotation in order to promote bubble clustering? The answer to this question appears to be that smaller bubbles, rather than larger bubbles should be generated, although the distinction between smaller and larger is difficult to quantify. The bubble sizing algorithm used in this study (and detailed in Leppinen & Dalziel (2004)) uses a contouring technique to measure bubble sizes, and the technique cannot be used to measure the size of overlapping bubbles. Instead, the contouring technique measures the size of isolated bubbles. The size distribution of these isolated bubbles changes as a function of location in the flotation tank, and the data is clearly consistent with smaller bubbles preferentially being incorporated into bubble clusters.

Table 1 presents statistics (minimum, maximum, median, arithmetic mean and standard deviation of the bubble diameter) from each of the measurement locations in the Albert study. (The statistics in Table 1 do not include the effect of macrobubbles—bubbles greater than 1,000 μm in diameter—which are discussed below.) All of the bubbles in the tank are generated by the pressure reduction nozzles in the contact zone; however, the bubble size distribution can change downstream in the flotation zone as bubble clusters and individual bubbles rise to the free surface. Indeed, the change in the bubble size distribution within the flotation zone is significant. The median bubble size at different depths in the contact zone varies between 70 and 84 μm. Within the flotation zone, the median bubble size at a depth of 0.15 m is comparable to that within the contact zone. At a depth of 0.7 m, the median bubble size in the flotation zone is approximately 70% larger than at a depth of 0.15 m. This large increase in the median bubble size with depth is statistically significant, and must be the result of a physical process in the flotation zone. It should be noted that the actual number of bubbles (both small and large) observed at a depth of 0.7 m is considerably lower than the number of bubbles at a depth of 0.15 m; however, the bubbles observed at a depth of 0.7 m are larger on average than the bubbles at a depth of 0.15 m. At a depth of 1.2 m, the bubble concentration is even smaller than at a depth of 0.7 m. The bubble sizes observed at a depth of 1.2 m were substantially smaller than those observed at 0.7 m, and comparable, although slightly larger, than those at a depth of 0.15 m.

Table 1 | Bubble size (diameter) statistics at different locations in the Albert study: s.d. refers to the standard deviation, and cluster refers to the average number of clusters per image. All bubble measurements are in microns and depth measurements are in metres

Location	Depth	Min	Max	Median	Mean	s.d.	Cluster
A	0.15	21	263	70	82	44	2.00
	0.70	49	270	75	119	37	2.10
	1.00	25	454	81	105	56	n.a.
	1.20	22	295	70	122	44	n.a.
	1.80	14	402	84	116	75	n.a.
B	0.15	17	375	72	87	51	1.90
	0.70	66	257	125	141	44	0.60
	1.20	57	134	105	106	20	0.00
C	0.15	14	295	67	80	44	1.70
	0.70	59	310	125	157	38	0.40
	1.20	56	120	89	90	15	0.15
D	0.15	20	291	71	85	48	1.50
	0.70	34	256	132	135	40	0.10
	1.20	57	166	106	111	18	0.02
E	0.15	20	287	81	96	50	1.30
	0.70	89	276	158	165	45	0.08
	1.20	57	152	120	117	22	0.03
F	0.15	20	334	90	105	42	1.15
	0.70	85	232	145	147	44	0.05
	1.20	75	156	110	124	20	0.00
G	0.15	27	270	90	106	50	0.98
	0.70	60	290	143	145	50	0.04
	1.20	38	127	93	92	22	0.01

The increase in the average bubble size at a depth of 0.7 m in the flotation zone can be explained in terms of bubble clustering: small bubbles are preferentially incorporated into bubble clusters. With reference to Figure 1, the trajectory of bubbles and bubble clusters in the flotation zone will depend on the rise velocities of the

bubbles (clusters), as well as the mean flow in the tank and turbulent fluctuations. Bubble clusters can have significantly higher velocities than individual bubbles (Leppinen *et al.* 2001) and this is consistent with the observation of few bubble clusters at depth (see Table 1). Smaller bubbles will have a slower rise velocity than larger bubbles, and it would seem more likely that the mean flow and turbulence will carry smaller bubbles to depth, than larger bubbles. The statistics, however, indicate that relatively few small bubbles are observed at depth. What has happened, then, to the smaller bubbles? The answer appears to be that smaller bubbles are preferentially incorporated into bubble clusters. These bubble clusters will have much greater rise velocities than individual bubbles and will be able to dominate the mean flow and turbulent fluctuations and rise to the sludge blanket. If large bubbles are not incorporated into clusters, then it is possible for the mean flow and turbulence to carry these bubbles to a depth of 0.7 m, even though these larger bubbles will have faster rise velocities than other, smaller, bubbles. At depths of 0.7 m and below there are relatively few bubble clusters for isolated bubbles to become incorporated into. Hence, any bubbles observed at a depth of 0.7 m, will either rise or fall, based on their individual, isolated rise speeds, with smaller bubbles having a greater likelihood of being carried downwards than larger bubbles. This explains the decrease in the average bubble size between a depth of 0.7 m and a depth of 1.2 m.

Another possible explanation for the increase of bubble size with depth in the flotation zone is bubble coalescence, with smaller bubbles coalescing together to form larger bubbles. Saffman & Turner (1956) have a developed a mathematical model that can be used to describe bubble coalescence. This model is described in the Appendix and it is concluded that bubble coalescence alone cannot be used to explain the trends in Table 1. In particular, while bubble coalescence does cause small bubbles to combine to form larger bubbles, it is statistically unlikely that coalescence will result in the increase in the median bubble sizes at a depth of 0.7 m noted in Table 1.

If bubble clusters act as nets, collecting bubbles and floc particles as they rise, why should smaller bubbles be preferentially incorporated into bubble clusters? The answer is probably not that smaller bubbles are preferentially incorporated into bubble clusters, but that larger bubbles are preferentially excluded. Consider the situation depicted in Figure 7, where there is a relatively large bubble contained in a bubble cluster. If there is a velocity shear near the cluster, there will be a hydrodynamic force acting on all of the bubbles in the cluster. This force will be proportional to the surface area of the bubbles, with the largest forces acting on the largest bubbles. It is conceivable that these forces will cause larger bubbles to break away from bubble cluster, carrying away a small amount of flocs. Indeed images similar to those in Figure 7 have been observed, with large bubbles apparently tearing clumps of flocs from bubble clusters.

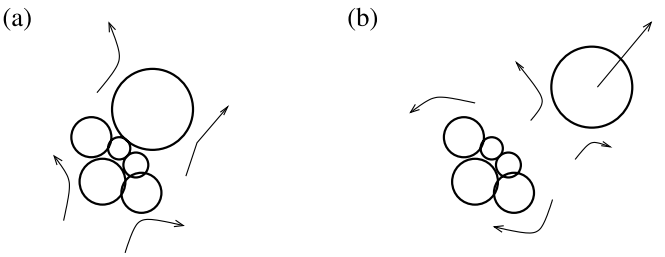

Figure 7 | A schematic of a large bubble detaching from a bubble cluster due to hydrodyamic forces acting on the large bubble.

Graincliffe study

Experience gained from the Albert study allowed for an increase in the amount of data which could be collected and processed from the Graincliffe Water Treatment Works. In total a fivefold increase in the number of bubble size measurements was achieved. The Graincliffe study provided convincing evidence of the importance of bubble clustering. Further the Graincliffe study allowed the opportunity to compare the performance of two different bubble generation techniques in otherwise identical conditions. Measurements were made in two flotation tanks: tank A was fitted with the same type of pressure reduction nozzle that was used at Albert and tank B was fitted with needle valves.

Macrobubbles

A visual inspection of the free surface of tank B near the contact zone suggested that macrobubble formation was a

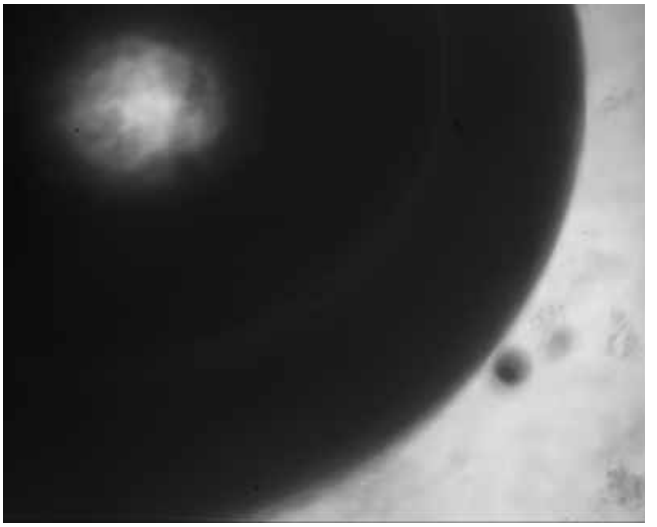

Figure 8 | A magnified image of a macrobubble. The image is 1.8 mm wide by 1.5 mm high.

serious problem with the needle valves. This was confirmed during the measurement study. A macrobubble can arbitrarily be defined as a bubble with a diameter of greater than 1 mm. Above it was argued that smaller bubbles are preferentially incorporated into bubble clusters, so on this basis, macrobubble formation should be avoided. Of greater concern are the costs associated with macrobubble formation. A 1 mm macrobubble contains the equivalent amount of air as one thousand 100 μm bubbles, while a 5 mm macrobubble contains the equivalent amount of air as 125,000 100 μm microbubbles. If the air that went into generating macrobubbles was effectively used to create microbubbles, then the overall recycle rate used during dissolved air flotation could be reduced, thus reducing the cost of running the saturation system.

Figure 8 shows a macrobubble measured at location 1 (i.e. near the tank inlet) at a depth of 0.2 m in tank B. The size of the macrobubble is estimated by first assuming that the bubble is spherical (which is not strictly true, but this is not of significance for the current purpose), and then by noting that the radius of a circular arc is uniquely specified by three points along its perimeter. Using this technique, the macrobubble in Figure 8 is estimated to have a diameter of 2.9 mm. In all, 2,000 images were analysed at this measurement point and 148 macrobubbles were observed. These macrobubbles contained enough air to form over 4 million 100 μm microbubbles (the equivalent of over 2,000 microbubbles per image). This number should be compared with the approximately 17,000 bubbles ranging from 16 to 350 μm which were actually observed in the 2,000 images at this location. Clearly macrobubble formation is a significant problem with the needle valves in tank B. The amount of macrobubbles produced by the Albert nozzles in tank A was also measured and was seen to be only 15% of that produced by the needle valves in tank B.

It is important to note that the formation of macrobubbles in tank B was a transient phenomenon, perhaps associated with the needle valves becoming blocked and then unblocked. This transience was easily observed by examining the water which was being syphoned through our measurement cylinder. At times the water was nearly opaque, indicating the presence of a large number of microbubbles, while at other times the water was nearly transparent, indicating relatively few microbubbles, with macrobubbles clearly visible. We did not systematically study the transition between these two regimes, but it is clear that the bubble size distribution within the flotation tank as a whole will depend on the relative time spent in each regime.

Bubble size distributions

The bubble size distribution was determined at each of the measurement points in the Graincliffe study. The data is plotted in Figures 9–13 in terms of number fraction at each of the measurement locations. The data has been placed into bins which are 12 μm wide. The data point for bubble size equal to 6 μm represents the total number of bubbles at the given measurement location with a diameter between 0 and 12 μm divided by the total number of bubbles measured at that given measurement location (similarly for the data points for size equal to 18 μm, 30 μm, 42 μm, . . .). The most striking feature of Figures 9–12 is the general trend of a shift to larger bubble sizes when moving downstream from the tank inlet end to the over flow weir end. If the increase in bubble size were solely the result of bubble coalescence, the results in the Appendix would suggest that the peak in the bubble size

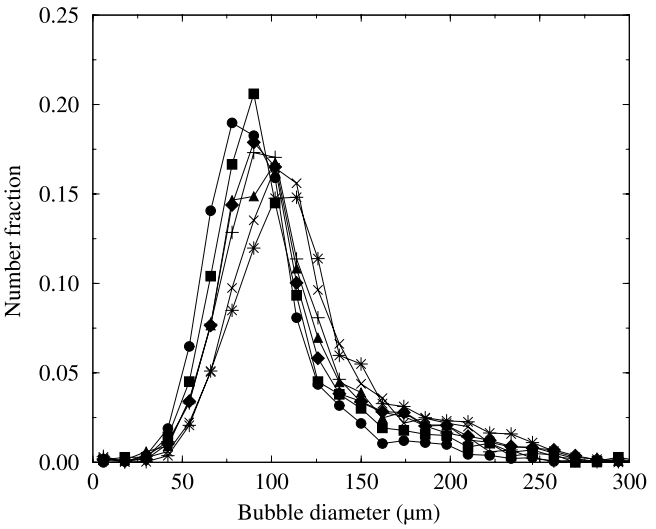

Figure 9 | Bubble size distribution in tank A at Graincliffe at a depth of 0.2 m at different measurement locations (see Figure 5): 3 (●); 4 (■); 5 (◆); 6 (▲); 7 (+); 8 (×); 9 (*).

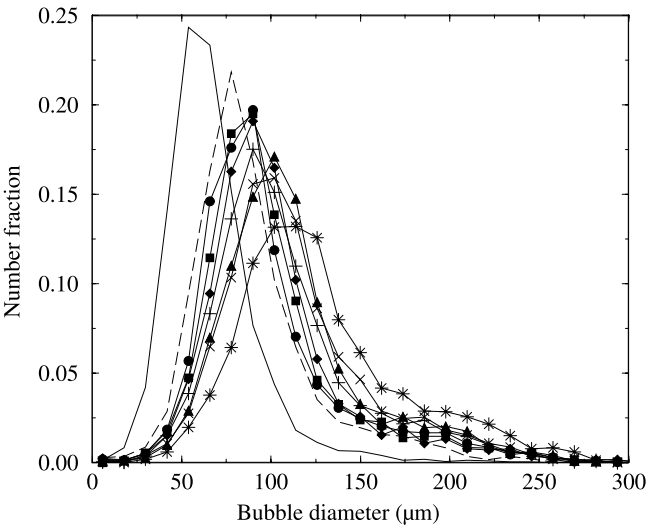

Figure 11 | Bubble size distribution in tank B at Graincliffe at a depth of 0.2 m at different measurement locations (see Figure 5): 1 (————); 2 (— — —); 3 (●); 4 (■); 5 (◆); 6 (▲); 7 (+); 8 (×); 9 (*).

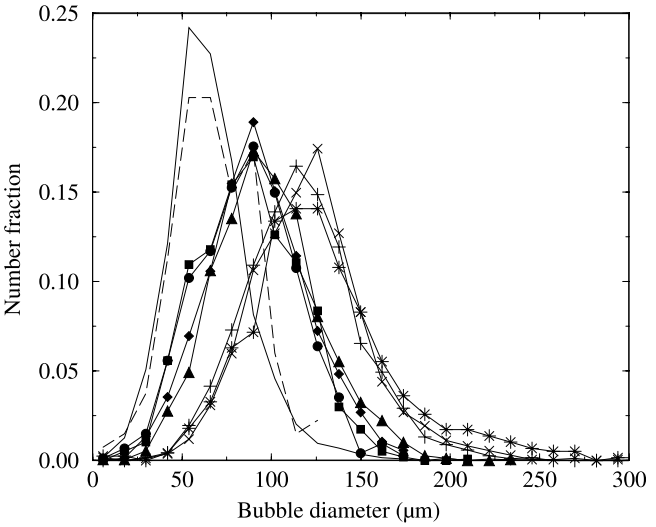

Figure 10 | Bubble size distribution in tank A at Graincliffe at a depth of 1.2 m at different measurement locations (see Figure 5): 1 (————); 2 (— — —); 3 (●); 4 (■); 5 (◆); 6 (▲); 7 (+); 8 (×); 9 (*).

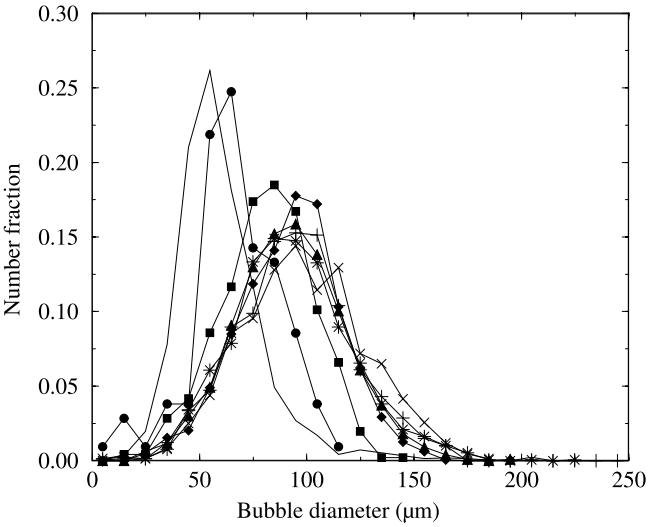

Figure 12 | Bubble size distribution in tank B at Graincliffe at a depth of 1.2 m at different measurement locations (see Figure 5): 1 (————); 3 (●); 4 (■); 5 (◆); 6 (▲); 7 (+); 8 (×); 9 (*).

distribution should move towards smaller bubble sizes. The observation that the peak in the bubble size distribution shifts towards larger bubble sizes, indicates that some mechanism, other than bubble coalescence, must be responsible for removing smaller bubbles from the bubble population. It is hypothesized that this mechanism is the preferential incorporation of smaller bubbles into bubble clusters. As smaller bubbles are incorporated into clusters within the flotation zone, it is the larger bubbles which remain. The largest exception to the observation that bubble size tends to increase when moving downstream from the tank inlet, is given by the size distributions for

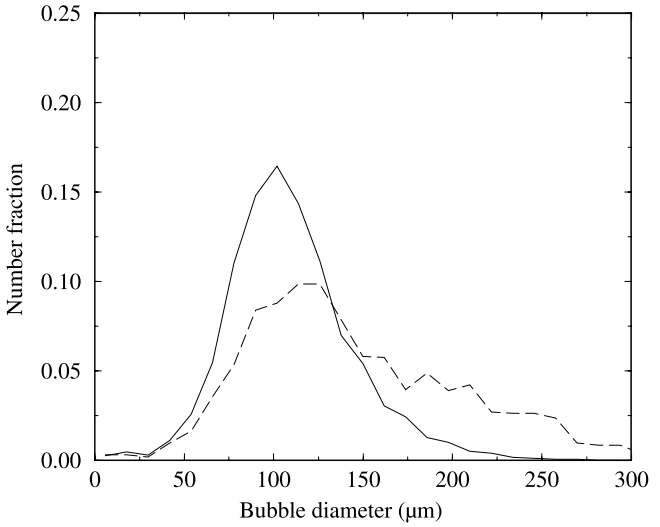

Figure 13 | Bubble size distribution in tank B at Graincliffe at a depth of 0.2 m at different measurement locations (see Figure 5): 1 (————); 2 (— — —).

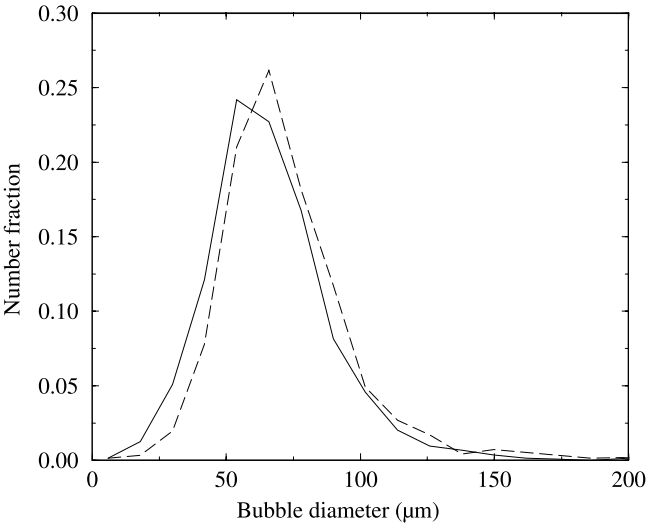

Figure 14 | A comparison of the bubble size distributions at Graincliffe at a depth of 1.2 m: tank A (————); tank B (— — —).

bubbles measured at locations 1 and 2 in tank B at a depth of 0.2 m. It is felt that these size distributions are skewed, possibly due to blocked needle valves, and the resultant formation of macrobubbles. It is for this reason that these size distributions are plotted by themselves in Figure 13, instead of with the other size distributions for this tank at a depth of 0.2 m given in Figure 9. It has been noted that macrobubble formation is a transient phenomenon, and the measurements in the contact zone in tank B at a depth of 1.2 m did not indicate the presence of a significant fraction of macrobubbles. A direct comparison of the bubble sizes generated by the Albert nozzles in tank A and the needle valves in tank B is given in Figure 14 which plots the bubble size distributions in the contact zone at a depth of 1.2 m. Remarkably, when the needle valves in tank B are not blocked, they generate virtually the same size distributions of bubbles as the Albert nozzles in tank A.

At Graincliffe measurements were only performed at two depths, in comparison with the three depths surveyed at Albert. This compromise was made in order to make measurements in both tank A and tank B in the time allowed for the study. One consequence is that the pronounced increase in bubble size at a depth of 0.7 m observed at Albert, was not identified at Graincliffe where measurements were only made at a depth of 0.2 and 1.2 m. As noted above, bubble sizes at Albert at a depth of 1.2 m were comparable to those measured at a depth of 0.15 m. This is consistent with the comparable bubble sizes observed at Graincliffe at depths of 0.2 and 1.2 m.

Floc fragmentation

At both Albert and Graincliffe flocs are formed by flash mixing the raw water with a ferric sulphate coagulant, before conditioning in a two stage flocculation plant with a retention time of 20 minutes. The layout of the flocculation tanks at the Graincliffe Water Treatment Works made it easy to use the bubble size measurement instrumentation to visualize the flocs before they entered the flotation tank. The results indicate that flocs can come in a variety of shapes and sizes. In general the flocs are non-isotropic in shape with lengthscales in two dimensions being comparable and somewhat greater than the lengthscale in the third dimension. The flocs might best be described as relatively thick, irregularly shaped pancakes composed of tiny dendrites and floc monomers. Coherent flocs as large as 4 mm across were observed, as were flocs as small as 10 μm. Due to the irregular nature of the floc shape it was not possible to develop an algorithm to automatically

determine the floc size distribution. Instead, it has been observed by eye that a significant fraction of flocs are greater than 1 mm in size. This is in considerable contrast with the flocs observed in the flotation tanks which were typically only 100 μm in size. (As an aside it is noted that the observation of 4 mm flocs in the flocculator provides direct evidence that the bubble size measurement instrumentation used in this study cannot be responsible for the floc fragmentation observered in the flotation tank.) While it is difficult to quantify the exact extent of floc fragmentation, it is clear that significant fragmentation does occur. There are two possible implications of this observation. The first concerns the residence time in the flocculator: If large flocs are torn apart upon entry into the flotation tank, is it possible to reduce the time spent in the flocculator? Clearly there will still be a requirement for mixing of coagulants, etc. to prepare the flocs for flotation. The second concerns the efficiency of flotation. Bubble clustering appears to play a large role in flotation, and bubble clusters appear to be held together by large clumps of flocs. If this is indeed the case then floc fragmentation should be minimized in order to promote the formation of bubble clusters.

CONCLUSIONS

This paper has reported on two studies to measure bubble sizes in dissolved air flotation tanks operated by Yorkshire Water. Measurements were obtained by inserting a perspex tube at the desired location and depth in the flotation tank and withdrawing samples of water. An image processing system was then used to automatically measure bubble sizes. The results reported in this paper are thought to be the first direct measurements of bubble size in a full-scale flotation tank. By directly observing bubble/floc interaction, it is has been possible to identify the dominant processes controlling floc removal efficiency. A preliminary study was performed at the Albert Water Treatment Works where microbubbles are generated using a conventional pressure reduction nozzle. A second study was performed at the Graincliffe Water Treatment Works. In one tank at Graincliffe bubbles were generated using the same pressure reduction nozzles as those used at Albert, while in a second tank bubbles were generated using needle valves.

After bubbles are generated in the contact zone of a flotation tank they interact with floc particles and can either rise to the sludge blanket or they can be carried away with the exit flow stream in the flotation zone. Due to the fluid motion in the tank and due to bubbles rising to the sludge blanket, the size distribution of bubbles will vary as a function of location in the flotation tank. By examining changes in the size distribution within the tank, it is possible to identify processes which are important during flotation. During both the Albert and the Graincliffe studies, it was confirmed that bubble clusters play a significant role during flotation. A bubble cluster is a large group of bubbles which are all attached to the same clump of floc particles. The combined buoyancy of a large number of bubbles ensures that bubble clusters will have a large rise velocity so that they can successfully rise to the sludge blanket. As clusters rise, they act as nets, filtering isolated flocs or bubbles, and carrying them upwards. Bubble clusters are capable of removing significantly more floc particles than isolated bubbles and hence flotation efficiency can be increased by promoting the formation of bubble clusters. The results presented in this paper are significant because they provide the motivation for modelling bubble/floc interactions in a more realistic way than has previously been assumed (Han & Lawler 1991; Han *et al.* 1997; Leppinen 1999). Moreover, the results of this study suggest that bubble clusters can change their buoyancy outside of the contact zone of the flotation tank, a feature which has not been noted in previous models of flotation (Matsui *et al.* 1998; Fukushi *et al.* 1998; Leppinen 2000).

The results indicate that smaller bubbles are preferentially incorporated into bubble clusters. Bubbles larger than approximately 150 μm are less likely to be incorporated into bubble clusters than smaller bubbles, and the air used to generate these larger bubbles is not being used effectively. These conclusions offer clear guidance in developing design criteria for a pressure reduction nozzle which will enhance the efficiency of flotation. Nozzles should be designed to minimize macrobubble formation and to generate relatively small bubbles

(smaller than 150 μm) which are easily incorporated into bubble clusters. Ideally, the nozzle should be designed to produce a microbubble jet which is sufficiently weak that it will not lead to floc fragmentation in the contact zone. While previous studies have recommended the use of smaller bubbles in dissolved air flotation, this study provides the first direct measurement of bubble sizes in an actual flotation tank, as well as providing a physical explanation of why smaller bubbles are preferential.

APPENDIX

The simplest means of modelling bubble coalescence during dissolved air flotation is to use the turbulent coagulation theory developed by Saffman & Turner (1956). A population balance approach is then used to track the number density distribution as bubbles coalesce to form larger bubbles. Saffman & Turner (1956) have shown that the coalescence rate of spheres of size r_i and r_j is:

$$N_{ij} = \alpha n_i n_j (r_i + r_j)^3 \tag{A1}$$

where α is a rate constant and n_i (n_j) is the number density of bubbles of size r_i (r_j). The rate constant α depends on the strength of the turbulence which is inducing coalescence and it has been assumed that all bubble/bubble collisions will lead to coalescence. In realilty collision/coalescence efficiency will be affected by interparticle forces (Leppinen 1999) and the rate constant α is actually an increasing function of $r_i + r_j$. For simplicity we will assume that α is constant; however, this will not affect the conclusions reached in this appendix.

The rate of change of the number density of bubbles of size r_i is then

$$\frac{dn_i}{dt} = -2N_{ii} - \sum_{i \neq j} N_{ij} + F_i \tag{A2}$$

where F_i is the rate of formation of bubbles of size r_i given by

$$F_i = \sum_{r_j^3 + r_k^3 = r_i^3} N_{jk}. \tag{A3}$$

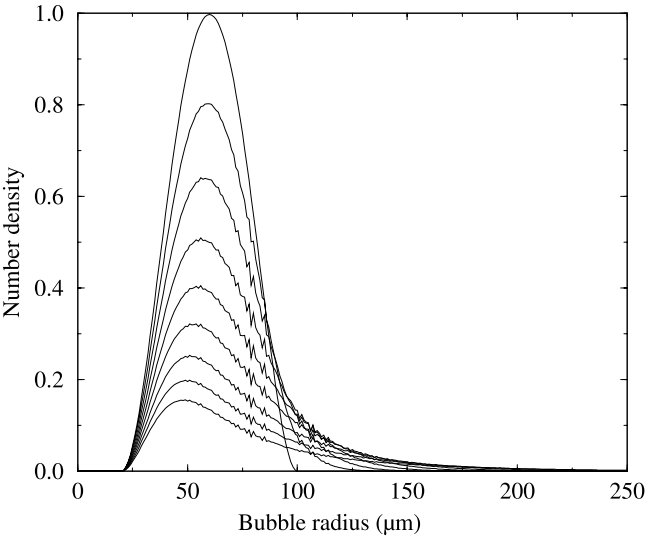

Figure 15 | The evolution in bubble number density distribution due to coalescence with time increasing from $\alpha t = 0$ to $\alpha t = 0.5$ as the peak number density decreases.

In practice a population balance model based on (A1) to (A3) is discretized by dividing the bubble size distribution into bins, centred at a radius r_i, of finite thickness. In this case, Equation (A3) must be suitably modified to ensure volume conservation.

Equations (A1) to (A3) show that bubble coalescence leads to a decrease in the concentration of smaller bubbles and an increase in the concentration of larger bubbles. The rates of change of the concentrations of the different size bubbles will depend on the respective bubble sizes. As an illustrative example, consider the initial bubble size distribution given in Figure 15 which has been discretized using 1 μm wide bins. The initial size distribution contains bubbles ranging in size from 20 to 100 μm and has a peak at 60 μm. The number densities have been normalized in such a way that the peak concentration is one bubble per unit volume. As time passes, the total number of bubbles decreases while the size of the maximum bubble increases. (The oscillations in the number density profiles at later times is a consequence of the finite size of the bins used during the discretization.) A significant feature is that the rate of decrease in the number of bubbles which are smaller than the peak bubble size is less than the rate of decrease in the number of bubbles which are greater than

the peak bubble size. As a consequence, the peak bubble size decreases with time. This trend can be understood by examining Equation (A1). If the number densities of bubbles of different sizes are comparable, then it is more likely for large bubbles to coalesce than for smaller bubbles, due to the cubic dependence of coalescence rate on radius.

The trends observed in Figure 15 are repeated for any sufficiently smooth and realistic initial bubble size distribution. The conclusion is that bubble coalescence leads to a relatively rapid increase in the concentration of larger bubbles, while there is a much smaller decrease in the concentration of smaller bubbles. Thus, it can be concluded that the increase in the minimum bubble size noted in Table 1 is not solely the result of bubble coalescence. It can be further concluded that the increase in the peak bubble sizes oberved in Figures 9–13 cannot be explained in terms of bubble coalescence.

REFERENCES

Dalziel, S. B. 2003 *Digiflow User's Guide*, technical report. University of Cambridge, Cambridge, UK.

Franklin, B., Wilson, D. & Fawcett, N. S. J. 1997 Ten years of experience of dissolved air flotation in Yorkshire Water. In *Proceedings of the 1997 London Conference on Dissolved Air Flotation*, April 1997. 141–160.

Fukushi, K., Matsui, Y. & Tambo, N. 1998 Dissolved air flotation: experiments and kinetic analysis. *J. Wat. Suppl.: Res. & Technol.—AQUA* **47**, 76–86.

Han, M., Dockko, S. & Park, C. 1997 Collision efficiency factor of bubble and particle α_{bp} in DAF. In *Proceedings of the 1997 London Conference on Dissolved Air Flotation*, April 1997. 409–416.

Han, M. Y. & Lawler, D. F. 1991 Interactions of two settling spheres: settling rates and collision efficiencies. *J. Hydraul. Eng. ASCE* **117**, 1269–1289.

Kiuru, H. J. 2001 Development of dissolved air flotation technology from the first generation to the newest (third) one (daf in turbulent flow conditions). *Wat. Sci. Technol.* **43**(8), 1–7.

Leppinen, D. M. 1999 Trajectory analysis and collision efficiency during microbubble flotation. *J. Coll. Int. Sci.* **212**, 431–442.

Leppinen, D. M. 2000 A kinetic model of dissolved air flotation including the effects of interparticle forces. *J. Wat. Suppl.: Res. & Technol.—AQUA* **49**, 259–268.

Leppinen, D. M. & Dalziel, S. B. 2004 Microbubble formation during dissolved air flotation (In preparation).

Leppinen, D. M., Dalziel, S. B. & Linden P. F. 2001 Modelling the global efficiency of dissolved air flotation. *Wat. Sci. Technol.* **43**, 159–166.

Matsui, Y., Fukushi, K. & Tambo, N. 1998 Modeling, simulation and operational parameters of dissolved air flotation. *J. Wat. Suppl.: Res. & Technol.—AQUA* **47**, 9–20.

Saffman, P. G. & Turner, J. S. 1956 On the collision of drops in turbulent clouds. *J. Fluid Mech.* **1**, 16–30.

First received 6 October 2003; accepted in revised form 15 June 2004